NIOBIAN CALCIOTANTITE AND PLUMBOAN-STANNOAN CESSTIBTANTITE FROM THE ISLAND OF UTÖ, STOCKHOLM ARCHIPELAGO, SWEDEN

STEN-ANDERS SMEDS

Department of Earth Sciences, Uppsala University, Villavägen 16, SE-752 36 Uppsala, Sweden

PETR ČERNÝ[1] AND RON CHAPMAN

Department of Geological Sciences, University of Manitoba, Winnipeg, Manitoba R3T 2N2, Canada

ABSTRACT

Niobian calciotantite and plumboan-stannoan cesstibtantite are associated with albite, K-feldspar, quartz and pink Ca-enriched tourmaline in the pollucite-bearing Grundberg outcrop of the northern Nyköpingsgruvan pegmatite on the island of Utö, Stockholm Archipelago, south-central Sweden. Cesstibtantite forms an overgrowth on subhedral, compositionally zoned grains of niobian calciotantite; both phases are locally intergrown with skeletal manganocolumbite, cassiterite and an unknown Ta-rich oxide phase. The maximum Nb content of the (Na,Pb)-poor calciotantite is as high as 19.90 wt.% Nb_2O_5 (1.263 *apfu* Nb, 31.6% of the *B*-site population). The (Pb,Sn,Nb)-enriched cesstibtantite averages at $(Pb_{0.35}Sb_{0.25}Sn_{0.10}Ca_{0.12}Na_{0.12})(Ta_{1.40}Nb_{0.55}W_{0.05})$ $(O_{5.70}[OH]_{0.30})([OH]_{0.66}Cs_{0.30})$. Low-temperature hydrothermal fluids triggered a unique two-stage alteration of cesstibtantite, leaving the other minerals intact. Diffuse cation-exchange spreads from microfractures in cesstibtantite. Gradual loss of Cs, Pb, Sb and Sn is compensated by progressive introduction of Ca, Na and Sr, and minor F substitutes for OH, but *B*-site cations are not affected. The resulting compositions attain $(Ca_{0.32}Na_{0.25}Sb_{0.25}Sn_{0.03}Pb_{0.20}Sr_{0.02})(Ta_{1.40}Nb_{0.55}W_{0.05})(O_{5.85}[OH]_{0.15})([OH]_{0.55}O_{0.10}$ $F_{0.10}Cs_{0.15})$. Extremely thin rims of the microfractures, 1 to 4 µm across, display much enhanced cation-exchange of the above type, combined with substantial fluorination, which generates secondary cesian microlite $(Ca_{0.80}Na_{0.40}Sb_{0.15}Sr_{0.05}Pb_{0.05}Sn_{0.02})$ $(Ta_{1.40}Nb_{0.55}W_{0.05})(O_{5.90}[OH]_{0.10})([OH]_{0.36}O_{0.15}F_{0.30}Cs_{0.10})$.

Keywords: calciotantite, cesstibtantite, microlite, electron-microprobe analysis, tantalum, niobium, cesium, granitic pegmatite, Utö Island, Sweden.

SOMMAIRE

Nous avons découvert un exemple de calciotantite niobifère et de cesstibtantite plombifère et stannifère en association avec albite, feldspath potassique, quartz et tourmaline rose enrichie en Ca dans un affleurement de pegmatite granitique à pollucite à Grundberg, dans la partie nord de la pegmatite de Nyköpingsgruvan, île de Utö, archipel de Stockholm, dans le secteur centre-sud de la Suède. La cesstibtantite se présente en surcroissance sur les cristaux sub-idiomorphes de calciotantite niobifère montrant une zonation. Les deux phases se présentent aussi en intercroissance avec la manganocolumbite squelettique, la cassitérite, et un oxyde méconnu riche en Ta. Les teneurs maximales en Nb dans la calciotantite à faible teneur en Na et Pb atteignent 19.90% de Nb_2O_5 en poids (1.263 atomes par unité formulaire de Nb, 31.6% du site *B*). La composition moyenne de la cesstibtantite enrichie en Pb, Sn et Nb est $(Pb_{0.35}Sb_{0.25}Sn_{0.10}Ca_{0.12}Na_{0.12})(Ta_{1.40}Nb_{0.55}W_{0.05})(O_{5.70}[OH]_{0.30})([OH]_{0.66}Cs_{0.30})$. Une phase fluide hydrothermale à faible température a causé une altération unique de la cesstibtantite en deux stades, sans affecter les autres minéraux. Un échange diffus de cations s'étend des microfractures dans la cesstibtantite. La perte en Cs, Pb, Sb et Sn est compensée par l'introduction progressive de Ca, Na et Sr, et un quantité mineure de fluor remplace l'hydroxyle, mais les cations dans la position *B* ne sont pas affectés. Les compositions qui résultent de cette transformation atteignent $(Ca_{0.32}Na_{0.25}Sb_{0.25}Sn_{0.03}Pb_{0.20}$ $Sr_{0.02})(Ta_{1.40}Nb_{0.55}W_{0.05})(O_{5.85}[OH]_{0.15})([OH]_{0.55}O_{0.10}F_{0.10}Cs_{0.15})$. Un liseré extrêmement étroit de 1 à 4 µm de largeur le long de microfractures montre un échange de ce même type et une fluorination plus avancés, pour mener à un microlite césique secondaire $(Ca_{0.80}Na_{0.40}Sb_{0.15}Sr_{0.05}Pb_{0.05}Sn_{0.02})(Ta_{1.40}Nb_{0.55}W_{0.05})(O_{5.90}[OH]_{0.10})([OH]_{0.36}O_{0.15}F_{0.30}Cs_{0.10})$.

(Traduit par la Rédaction)

Mots-clés: calciotantite, cesstibtantite, microlite, analyse par microsonde électronique, tantale, niobium, césium, pegmatite granitique, île de Utö, Suède.

---

[1]   *E-mail address*: p_cerny@umanitoba.ca

Introduction

Calciotantite, $CaTa_4O_{11}$, was discovered in granitic pegmatites of the Kola Peninsula by Voloshin et al. (1982). At a later date, a Na- and Pb-bearing variety of calciotantite was described as "ungursaite" from eastern Kazakhstan, Kola and the Democratic Republic of Congo by Voloshin et al. (1985), but the identity of this material with cesstibtantite was established by Yamnova et al. (1988).

Cesstibtantite also is a rare mineral, known from only five localities (Ercit et al. 1993). Thus the crystal-chemical and paragenetic aspects of any new occurrences of these minerals deserve close attention. Here we report on new occurrences of a Nb-rich calciotantite and of a Sn-enriched, plumboan cesstibtantite from the Nyköpingsgruvan granitic pegmatites on the island of Utö, in the Stockholm Archipelago, south-central Sweden, and on the unique products of alteration of the latter phase.

Background Information

Cesstibtantite, ideally $(Na,Sb)_{2-m}(Ta,Nb)_2(O>OH,F)_6$ $(OH,F;Cs>K)_{1-n}$, is a derivative of the pyrochlore group, and so far the only natural analog of synthetic inverse pyrochlores (Ercit et al. 1993), in which the populations of large-cation and (O,OH,F) sites are interchanged (Fourquet et al. 1973). Normal pyrochlores have a structural formula of $A_{2-m}B_2O_6\phi_{1-n}.pH_2O$, where the medium-radius A stands for Na, Ca (Ba, Bi, K,Pb, REE, Sb^{3+}, Sn^{2+}, Sr, Th, U, Y, Zr), the small-radius B stands for Nb, Ta and Ti (Sn^{4+}, Fe^{3+}), and ϕ stands for OH, F and O. In contrast, inverse pyrochlores have formulas of the type $\Box B_2O'_6A'$, with a vacancy $\Box$ in the A site of the normal pyrochlore structure, B corresponds to small R^{3+} to R^{6+} cations, O' represents O, OH and F, and A. represents large cations (r_i dominantly greater than 1.6 Å), namely Cs, Rb (Tl, K). Molecular H_2O may be present in both normal and inverse pyrochlores, hosted by either A or A' sites, or both. The H_2O molecules and the large cations A' may be displaced from the ideal positions (e.g., Jäger et al. 1959, Harris 1965, Groult et al. 1982, Ehlert et al. 1988, Ercit et al. 1994). The structure refinement of natural cesstibtantite shows that the mineral is intermediate between the normal and inverse pyrochlores, with the ϕ (A') site occupied by both anions and Cs (Ercit et al. 1993).

The Parent Pegmatite and Mineral Assemblage

The Nyköpingsgruvan dikes correspond to the petalite subtype of complex rare-element granitic pegmatites (cf. Černý 1991 for classification). At these classic localities, the magma was intruded into an iron-formation host rock (dominantly magnetite). Four new mineral species have been discovered over the past two centuries, and new assemblages are still being found (e.g., Langhof & Holtstam 1994). The pegmatites were recently characterized by Smeds & Černý (1989, and references therein) and reviewed by Teertstra et al. (1996) in the context of a re-examination of pollucite, first described by Smeds & Černý (1989).

Calciotantite and cesstibtantite were identified in two hand specimens from the Grundberg outcrop, an offshoot of the northern Nyköpingsgruvan pegmatite. This outcrop is so far the only location at which pollucite was found. The outcrop consists of an extremely leucocratic assemblage of albite, quartz, and K-feldspar, with minor pink tourmaline and accessory pollucite, apatite, blue tourmaline, and potassic to Rb-rich low-temperature K-feldspar (Teertstra et al. 1998).

In both hand specimens, the calciotantite and cesstibtantite are associated with fine- to medium-grained albite, quartz, K-feldspar and pink Ca-enriched elbaite to rossmanite. Cesstibtantite forms anhedral grains and subhedral crystals up to 1.5 mm in size, which enclose a microscopic core of calciotantite (Fig. 1). The calciotantite contains minor inclusions of
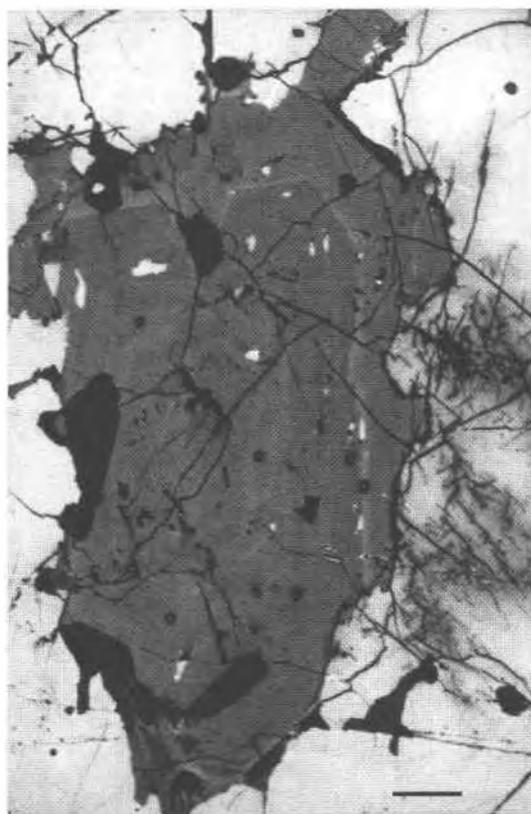

FIG. 1. Subhedral calciotantite (grey) with fine-scale concentric zoning of variable Ta and Nb contents, enclosed in cesstibtantite (white). Cassiterite (black) and cesstibtantite (white) form inclusions in calciotantite. Back-scattered-electron image. The scale bar is 100 μm long.

cassiterite and cesstibtantite, the latter populating in part specific concentric growth-zones of the host (Fig. 1). Both calciotantite and cesstibtantite are locally intergrown with skeletal manganocolumbite ($Mn_{3.41}$ $Fe_{0.46}Ca_{0.05}Mg_{0.01})(Nb_{5.22}Ta_{2.78}W_{0.02})O_{24}$, cassiterite containing 1.54 to 7.48 wt.% Nb_2O_5 and 1.36 to 13.60 wt.% Ta_2O_5 (Fig. 2). A few grains 3 to 6 µm across of an unknown phase consist of ~96 wt.% $(Ta>>Nb)_2O_5$ and give low analytical totals of ~97 to 98 wt.% (possibly lithiotantite, or unknown phases containing OH or H_2O). Diffuse alteration of cesstibtantite spreads out from microscopic fractures, which are marked by extremely fine veinlets of secondary microlite (Fig. 3); however, the other Ta,Nb-bearing phases are not affected.

EXPERIMENTAL

Calciotantite, cesstibtantite and the alteration products were analyzed with a Cameca SX–50 electron microprobe using wavelength-dispersion analysis at 15 kV and 20 nA, with a beam diameter of 1 to 2 µm. Counting time was 20 s for Na$K\alpha$ (microlite), Ca$K\alpha$ ($CaNb_2O_6$), Ta$L\alpha$ (manganotantalite), and Nb$L\alpha$ ($MnNb_2O_6$), 40 s for K$K\alpha$ (orthoclase), Cs$L\alpha$ (pollucite), Sr$L\alpha$ ($SrBaNb_4O_{10}$), Pb$M\beta$ (mimetite), Sb$L\alpha$ (stibiotantalite), Bi$M\beta$ ($BiTaO_4$), Sn$L\alpha$ (SnO_2), U$M\beta$ (UO_2), and Si$K\alpha$ (diopside), and 50 s for F$K\alpha$ (microlite), Ba$L\alpha$ ($Ba_2NaNb_5O_{15}$), Fe$K\alpha$ ($FeNb_2O_6$), Mn$K\alpha$ ($MnNb_2O_6$), Ti$K\alpha$ (TiO_2) and W$L\alpha$ ($CaWO_4$). Data reduction was performed using the PAP procedure of Pouchou & Pichoir (1985).

In the absence of analytical determination of H_2O^+, the anion contents of cesstibtantite and secondary cesian
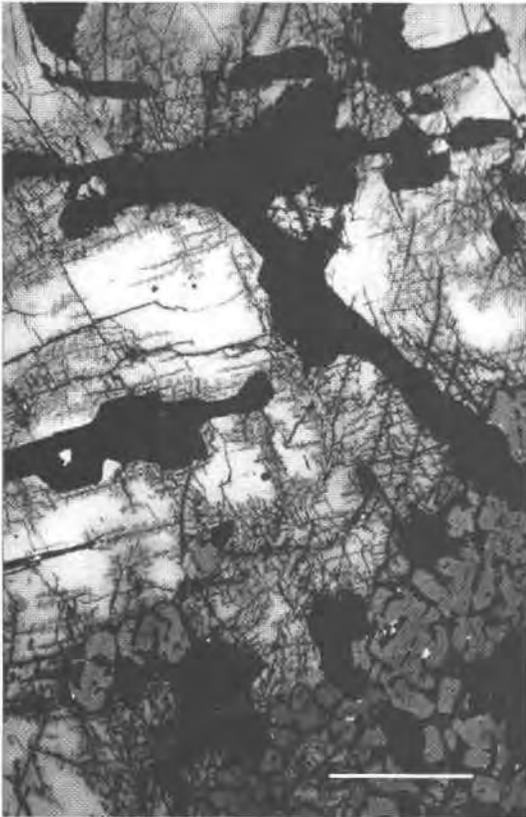

FIG. 2. A core of calciotantite (grey, lower right) in cesstibtantite (white), both intergrown with a fine to coarse skeletal network of manganocolumbite and cassiterite (black). Fine veinlets of secondary cesian microlite (black) penetrate cesstibtantite, surrounded by grey cation-exchanged haloes. Back-scattered-electron image. The scale bars is 200 µm long.
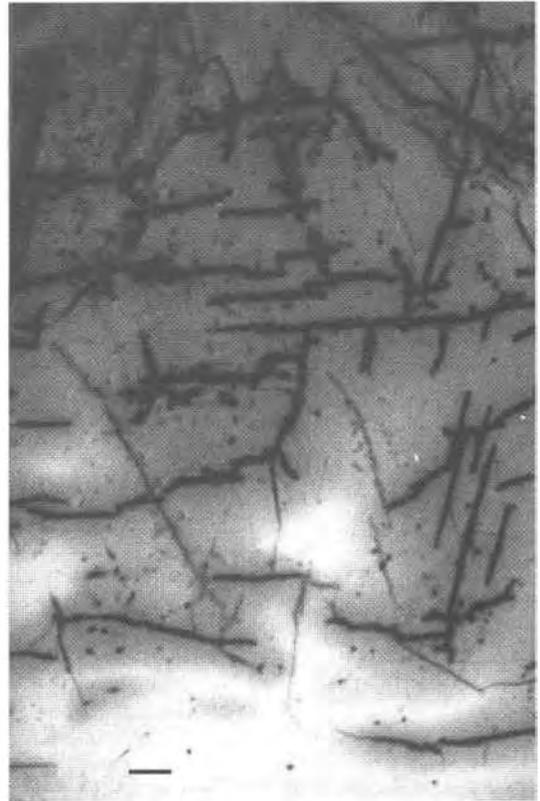

FIG. 3. Cesstibtantite (white) is progressively impoverished in Cs, Pb and Sn, and enriched in Ca, Na and F (darkening toward the top). The ion exchange has spread from microfractures occupied by secondary, F-rich cesian microlite (black veinlets). Back-scattered-electron image. The scale bars is 50 µm long.

microlite were calculated by the method devised by Ercit *et al.* (1993), based on structure refinement of cesstibtantite and on a model structure of $CsNb_2O_5F$ by Fourquet *et al.* (1973). (1) The number of OH groups at the O' site was matched to the number of Cs at the ϕ site to achieve local charge-balance, and the remainder of anion charge was calculated as (O,OH) complementary to F in the ϕ site. (2) The low analytical totals suggest up to 2.5 wt.% H_2O over and above H_2O required for calculated (OH) contents, indicative of the potential presence of molecular H_2O. However, the quantity of electrostatically neutral H_2O and its structural role cannot be estimated. Consequently, molecular H_2O was ignored, although it must have a significant effect on structural allocation of the charge-balancing (OH) groups. (3) The Sn content of cesstibtantite was calculated as SnO, on the basis of the composition of stannomicrolite (Ercit *et al.* 1987) and established convention for microlite and cesstibtantite (Ercit *et al.* 1993). (4) The Sb content was treated as trivalent. Some Sb^{5+} is perhaps geochemically possible, but the speculations of Voloshin *et al.* (1981) and the crude crystal-structure data of Gorogotskaya *et al.* (1996) do not prove its presence. Ercit *et al.* (1993) did not find any evidence for Sb^{5+}.

For cesstibtantite and microlite, X-ray powder-diffraction data were collected on the Nicolet D–5000 diffractometer in transmission mode, using CaF_2 (a = 5.465397 ± 4 Å) as an internal standard. Single-crystal X-ray-diffraction data obtained on a Siemens *P*4 automated four-circle diffractometer, with graphite-monochromated Mo$K\alpha$ radiation (λ = 0.71073 Å), were used to verify the identity and to refine unit-cell dimensions of calciotantite.

PRIMARY PHASES:
CALCIOTANTITE AND CESSTIBTANTITE

Calciotantite forms subhedral grains that show fine-scale oscillatory zoning of Nb and Ta contents (Fig. 1). The Nb content is variable, between 23.8 and 31.6 *apfu* (atoms per formula unit), much higher than previously recorded (13.7 *apfu* in "ungursaite"; Voloshin *et al.* 1985). Otherwise, no other elements enter the structure of our calciotantite in significant amounts. The contents of Na and Pb are very low, and the overall compositions yield formulae with near-perfect stoichiometry (Table 1).

Cesstibtantite is nearly homogeneous in back-scattered-electron (BSE) images, but moderate patchy variations were observed in the contents of Cs, Pb, Sb, Ta and Nb (Figs. 4A to D). Representative compositions given in Table 2 reflect this variability. Fluorine is in most cases below the detection limit (~0.07 wt.%) at the analytical conditions quoted above. Compared to the composition of cesstibtantite from previously examined localities, the Grundberg mineral is distinguished by

prominent contents of Pb (≤14.50 wt.% oxide, 0.390 *apfu*; Fig 4B) and remarkable but highly variable Sn (≤5.52 wt.% oxide, 0.244 *apfu*; Fig. 4D), both of which significantly surpass those established earlier (Voloshin *et al.* 1981, Ercit *et al.* 1993). The Nb content matches that of the most niobian compositions analyzed to date (Novák & Šrein 1998).

Limited quantities of the multiphase aggregates permitted identification of cesstibtantite, manganocolumbite and cassiterite by X-ray powder diffraction, but precise determination of unit-cell dimensions was not possible. However, doublets of microlite-type diffraction maxima indicate the presence of two cubic phases with *a* of about 10.54 Å (cesstibtantite) and 10.42 Å (secondary microlite, discussed below). For the single crystal of calciotantite, unit-cell dimensions in the hexagonal system were refined [*a* 6.2244(4), *c* 12.2772(10) Å], close to the values given by Voloshin *et al.* (1982); a structure refinement is in progress.

TABLE 1. REPRESENTATIVE COMPOSITIONS OF NIOBIAN CALCIOTANTITE FROM UTÖ, SWEDEN

		JL12	5JL17	JLG2D	2LG35	JL18
Nb_2O_5, wt%		19.90	18.40	15.80	14.40	13.97
Ta_2O_5		71.72	73.10	77.20	77.30	77.06
TiO_2		<0.01	<0.01	<0.01	<0.01	0.03
UO_2		0.04	0.00	0.03	0.05	0.00
Sb_2O_3		0.02	<0.02	<0.02	<0.02	0.03
Bi_2O_3		<0.01	0.09	<0.01	0.03	0.04
PbO		0.22	0.21	0.63	0.33	0.43
SnO_2		0.48	0.19	0.05	0.04	0.14
FeO		0.00	0.00	0.03	0.02	0.00
MnO		0.02	0.06	0.06	0.01	0.02
CaO		6.73	6.64	6.09	6.42	6.42
BaO		<0.04	<0.04	<0.04	<0.04	0.11
Na_2O		0.01	0.02	0.07	<0.01	0.03
K_2O		0.02	<0.01	0.04	0.01	0.00
Total		99.16	98.71	100.00	98.61	98.28
Atomic contents* (*apfu*)						
A	Na	0.003	0.006	0.010	-	0.008
	K	0.003	-	0.004	0.002	-
	Ca	1.005	1.005	0.930	0.998	1.002
	Ba	-	-	-	-	0.006
	Fe^{2+}	-	-	0.004	0.002	-
	Mn	0.002	0.008	0.008	0.002	0.002
	Pb	0.008	0.008	0.048	0.012	0.018
	Sb	0.002	-	-	-	0.002
	Bi	-	0.004	-	0.002	0.002
	U	0.001	-	0.001	0.002	-
Σ*A*		1.024	1.031	1.005	1.020	1.040
B	Ta	2.716	2.806	2.989	3.047	3.055
	Nb	1.253	1.174	1.018	0.944	0.920
	Sn^{4+}	0.026	0.012	0.004	0.002	0.008
	Ti	-	-	-	-	0.003
Σ*B*		3.995	3.992	4.011	3.993	3.986

* Normalized to 11 atoms of oxygen per formula unit; W, Si, Sr, Cs and F are below detection limits.
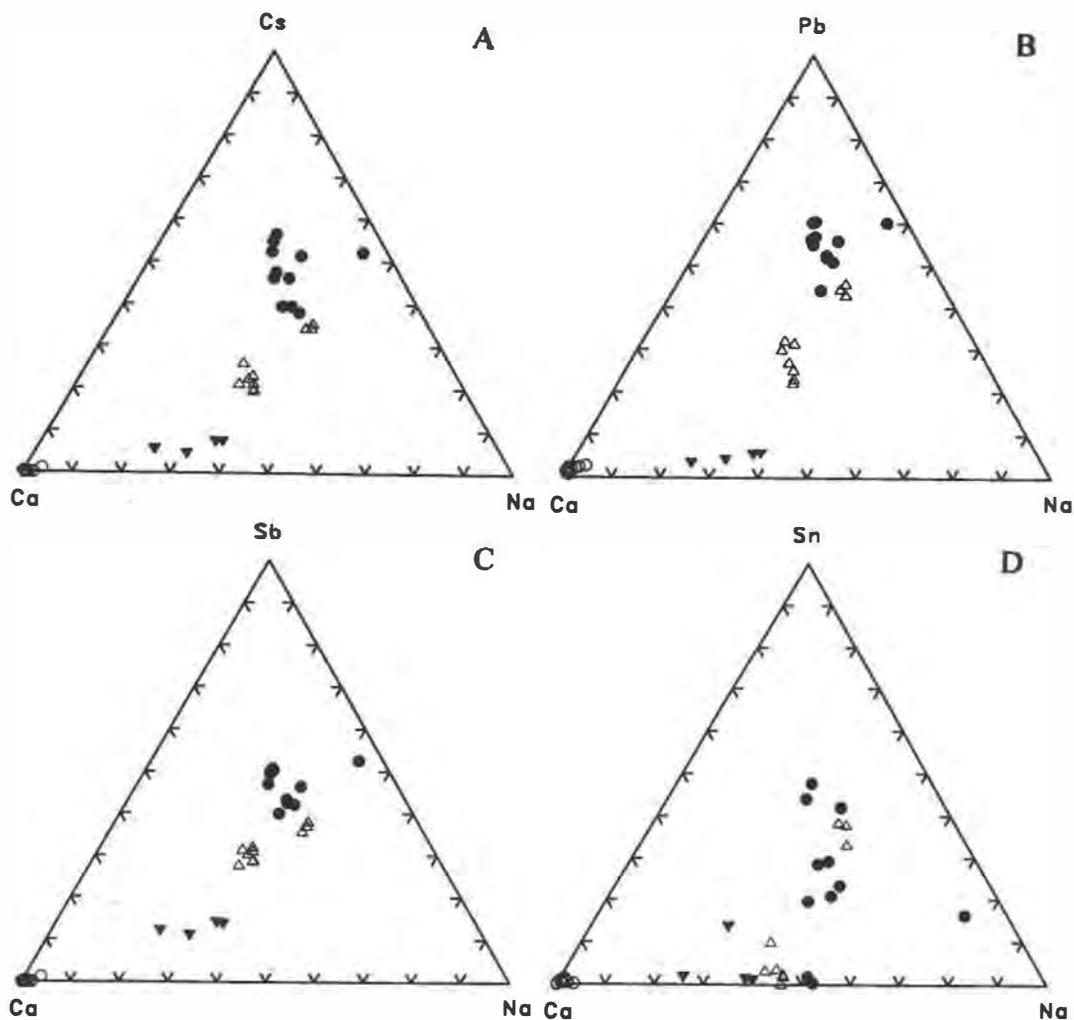
FIG. 4. Triangular plots of Ca–Na–Cs (A), Ca–Na–Pb (B), Ca–Na–Sb (C) and Ca–Na–Sn (D), in atomic proportions. Open circles: calciotantite; solid dots: cesstibtantite, open triangles: cesstibtantite affected by diffuse cation-exchange; inverted solid triangles: secondary cesian microlite.

ALTERATION PRODUCTS OF CESSTIBTANTITE: CATION AND ANION EXCHANGE

Diffuse darkening of cesstibtantite in the BSE images is caused by gradual loss of Cs, Pb, Sn and Sb (Figs. 2, 3). In contrast, Ca and Na show distinct enrichment; Sr, F and possibly Ba slightly increase, whereas Sb may locally behave erratically, and Ta, Nb and W are virtually constant (Table 2).

The cation exchange typical of the above diffuse alteration is much more extensive in the secondary cesian microlite that decorates the microfractures. The contents of Cs, Pb and Sn are greatly reduced, as is that of Sb (Fig. 4). In contrast, Ca, Na and F are considerably en-

riched, minor Sr and Si are introduced, and levels of U locally are close to the detection limit (~0.10 wt.% UO_2). No significant change is observed in the levels of Ta, Nb or W (Table 2).

GENETIC CONSIDERATIONS

At Utö, the occurrences of calciotantite and cesstibtantite are restricted to the Grundberg offshoot of the northern Nyköpingsgruvan dike. It is significant that this offshoot is the only member of the pegmatite swarm to be hosted by marble, and to contain pollucite.

Stabilization of the Grundberg calciotantite could have been triggered by contamination of the pegmatite-

forming melt by Ca from the host rock. This hypothesis is supported by the Ca-enriched composition of tourmaline (calcic elbaite to rossmanite, and liddicoatite along contacts), which also is restricted to the Grund-

TABLE 2. REPRESENTATIVE COMPOSITIONS OF NIOBIAN CESSTIBTANTITE AND ALTERATION PRODUCTS, UTÖ, SWEDEN

	cesstibtantite				cation-exchanged cesstibtantite				secondary microlite	
	LG 35B	JL1 BC	4LG 35	11JL 13	10JL 13	9JL 13	8JL 13	6JL 13	4JL 13	2JL 13
WO₃	1.88	2.39	1.75	2.33	2.32	2.49	2.48	2.49	2.51	1.90
Nb₂O₅	10.90	13.30	10.50	13.10	13.80	14.00	13.70	13.70	14.90	14.40
Ta₂O₅	54.10	49.10	54.20	50.70	50.50	52.40	52.60	53.30	55.30	56.70
SiO₂	<0.02	<0.02	<0.02	<0.02	<0.02	<0.02	<0.02	<0.02	<0.02	0.53
TiO₂	0.03	<0.01	<0.01	<0.01	<0.01	<0.01	<0.01	0.03	<0.01	<0.01
UO₂	<0.10	<0.10	<0.10	<0.10	<0.10	<0.10	<0.10	<0.10	<0.10	0.20
Sb₂O₃	6.98	5.51	7.07	5.54	6.18	6.46	7.08	7.52	5.66	4.52
Bi₂O₃	0.01	0.01	<0.01	<0.01	<0.01	0.03	<0.01	<0.01	<0.01	0.08
PbO	13.40	12.70	13.80	12.30	11.30	10.20	9.13	8.11	3.16	1.89
SnO	1.61	4.58	0.03	4.52	3.44	1.42	0.54	0.31	0.47	0.59
FeO	<0.01	0.02	<0.01	<0.01	<0.01	<0.01	<0.01	0.02	<0.01	0.05
MnO	<0.01	0.03	<0.01	0.04	0.07	0.12	0.09	0.08	0.05	0.11
CaO	1.33	0.99	1.26	1.18	1.64	3.11	3.47	3.88	8.14	9.25
SrO	<0.01	<0.01	0.01	<0.01	0.22	0.52	0.56	0.83	0.88	1.31
BaO	0.04	<0.03	<0.03	<0.03	0.07	0.05	0.03	<0.03	0.06	0.00
Na₂O	0.78	0.61	0.76	0.67	1.07	1.29	1.55	1.84	2.80	1.74
K₂O	0.04	0.03	0.04	0.07	0.03	0.06	0.04	0.04	0.01	0.00
Cs₂O	5.91	6.79	5.98	6.61	5.87	4.81	4.52	4.36	2.77	1.91
F	<0.07	<0.07	<0.07	0.09	0.11	0.25	0.28	0.29	1.32	1.00
–O=F	–	–	–	–0.04	–0.05	–0.11	–0.12	–0.12	–0.56	–
Total	97.00	96.06	95.40	97.01	96.57	97.10	95.95	96.68	97.47	95.79

Atomic contents per formula unit*

		LG 35B	JL1 BC	4LG 35	11JL 13	10JL 13	9JL 13	8JL 13	6JL 13	4JL 13	2JL 13
A	Na⁺	0.150	0.118	0.151	0.128	0.202	0.136	0.284	0.334	0.484	0.294
	Ca	0.142	0.106	0.139	0.125	0.171	0.314	0.352	0.390	0.778	0.866
	Sr	–	–	0.001	–	0.012	0.028	0.031	0.045	0.046	0.066
	Ba	0.002	–	–	–	0.003	0.002	0.001	–	0.002	–
	Fe²⁺	–	0.002	–	–	–	–	–	–	–	0.004
	Mn	–	0.003	–	0.003	0.006	0.010	0.007	0.006	0.004	0.008
	Pb	0.358	0.342	0.381	0.326	0.296	0.259	0.233	0.205	0.076	0.044
	Sn²⁺	0.071	0.204	0.001	0.199	0.149	0.060	0.023	0.013	0.019	0.023
	Sb	0.286	0.227	0.299	0.225	0.248	0.251	0.276	0.291	0.208	0.162
	Bi	–	–	–	–	–	0.001	–	–	–	0.002
	U	–	–	–	–	–	–	–	–	–	0.004
ΣA		1.009	1.002	0.972	1.006	1.087	1.161	1.207	1.286	1.617	1.473
B	Ta	1.462	1.336	1.513	1.358	1.335	1.343	1.353	1.359	1.341	1.344
	Nb	0.490	0.602	0.487	0.584	0.607	0.596	0.586	0.581	0.601	0.567
	W	0.048	0.062	0.047	0.057	0.058	0.061	0.061	0.060	0.058	0.043
	Ti	0.002	–	–	–	–	–	–	0.002	–	–
	Si	–	–	–	–	–	–	–	–	–	0.046
O₆'	O	5.745	5.706	5.733	5.713	5.753	5.800	5.813	5.821	5.894	5.929
	OH	0.255	0.294	0.267	0.287	0.247	0.200	0.187	0.179	0.106	0.071
φ	O	–	0.060	0.172	0.028	0.018	–	0.028	0.134	0.332	0.036
	OH	0.753	0.646	0.561	0.657	0.701	0.722	0.701	0.601	0.190	0.614
	F	–	–	–	0.028	0.034	0.075	0.084	0.086	0.372	0.276
A'	Cs	0.250	0.290	0.262	0.278	0.243	0.193	0.182	0.174	0.105	0.071
	K	0.005	0.004	0.005	0.009	·0.004	0.007	0.005	0.005	0.001	–

* See "Experimental" for the method of calculation and ion assignment. The electron-microprobe data are reported in weight %.

berg outcrop; in the main dikes, tourmaline is very Ca-poor (J.B. Selway, pers. commun., 1998). The effect of imported Ca could have been compounded by low activity of Fe and Mn in the very leucocratic host-rock (*cf.* Fig. 2 in Lumpkin & Ewing 1992). Voloshin *et al.* (1981, 1985) did not provide details of the geological setting of calciotantite- and "ungursaite"-bearing pegmatites; thus, a comparison with other occurrences of calciotantite is not possible in this respect.

Highly fractionated rare-element granitic pegmatites of the peraluminous LCT family (*cf.* Černý 1991 for classification) constitute the parent rocks at all localities of cesstibtantite known to date: Leshaia, Kola Peninsula in Russia (Voloshin *et al.* 1981), Tanco in Manitoba (Ercit & Černý 1982, Ercit *et al.* 1985), Mt. Holland, western Australia (Nickel & Robinson 1985), Dobrá Voda and Laštovičky, western Moravia, Czech Republic (Ercit *et al.* 1993, Novák & Šrein 1998). Leshaia and Tanco are the only pegmatites also to carry pollucite; however, this mineral could easily have remained unrecognized at some of the other localities.

Voloshin *et al.* (1981) assigned the formation of calciotantite and cesstibtantite to a late period of orthoclase-generating metasomatism, closely connected with replacement of pollucite, lepidolite and primary minerals of Nb and Ta, including stibiotantalite. According to these authors, Cs, Ta and Sb mobilized during this metasomatism yielded the late cesstibtantite. Such a process cannot be applied to the origin of cesstibtantite in either Nyköpingsgruvan or Tanco pegmatites. Stibiotantalite is so far unknown in Tanco and in the Grundberg outcrop. Cesstibtantite is a widespread ore mineral in the Tanco deposit, restricted to units that apparently preceded the crystallization of pollucite. In the Grundberg outcrop, cesstibtantite is generally associated with fine grains of pollucite, in aggregates indicative of virtually simultaneous crystallization of calciotantite, cesstibtantite, quartz, albite and pollucite. The only alteration of pollucite is partial cation-exchange to give analcime; this is a very low-temperature process that liberates Cs, but undoubtedly only after the crystallization of cesstibtantite. In both Tanco and Grundberg pegmatites, K-feldspar is present as relics of a primary phase, and as adularia replacing pollucite that is spatially separated from cesstibtantite and calciotantite. Consequently, cesstibtantite in the Tanco and Grundberg pegmatites must be considered a primary phase relative to their host assemblages; alteration of pre-existing minerals could not contribute any components to their precipitation.

The diffusive cation-exchange in the Grundberg cesstibtantite, leading to the introduction of Ca and Na and leaching of Cs, Pb, Sb and Sn, is unique among the six occurrences of this mineral known to date. Such exchange can be correlated, to a degree, with the secondary introduction of Ca into the pegmatite-hosted members of the pyrochlore group in general, as recognized by Lumpkin *et al.* (1986), Wise & Černý (1990) and Lumpkin & Ewing (1992, 1995), among others.

However, the fluorination of cesstibtantite (which is so prominent particularly in secondary cesian microlite from the microveinlets) seems to be a unique process, not observed in previous studies of pyrochlore-type minerals. Quite to the contrary, early F-bearing microlite tends to be increasingly hydroxylated in alteration processes, commonly leading to the total removal of fluorine (Lumpkin *et al.* 1986, Ohnenstetter & Piantone 1992, Lumpkin & Ewing 1992, 1995, and unpubl. data of M. Novák and P. Černý). It remains to be seen whether this late enrichment in F also occurs in other members of the microlite subgroup elsewhere in the Nyköpingsgruvan dikes. So far, rare minor veinlets of fluorite are the only other indication of late activity of fluorine.

The behavior of Nb, Ta and W supports the contention of Lumpkin (1989), Lumpkin & Ewing (1992) and Ercit *et al.* (1993), among others, that the *B*-site cations constitute a firm, fully populated framework in pyrochlore-type compounds, which is, under most circumstances, inert to cation exchange. The values of the atomic ratio $Ta/(Ta + Nb)$ in cation-exchanged cesstibtantite and secondary cesian microlite are all within the rather narrow range determined for the pristine cesstibtantite, 0.63 to 0.76. In contrast, the extensive leaching of Sn (concurrent with that of Cs and Pb) strongly supports its allocation to the *A*-site in the divalent state, as proposed for stannomicrolite by Ercit *et al.* (1987).

REFERENCES

ČERNÝ, P. (1991): Rare-element granitic pegmatites. I. Anatomy and internal evolution of pegmatite deposits. *Geosci. Canada* **18**, 49-67.

EHLERT, M.K., GREEDAN, J.E. & SUBRAMANIAN, M.A. (1988): Novel defect pyrochlores $ABi_2B_5O_{16}$ (A = Cs, Rb, B = Ta,Nb). *J. Solid State Chem.* **75**, 188-196.

ERCIT, T.S. & ČERNÝ, P. (1982): The paragenesis of simpsonite. *Geol. Assoc. Can. – Mineral. Assoc. Can., Program Abstr.* **7**, 48.

_____, _____ & HAWTHORNE, F.C. (1985): Normal and inverse pyrochlore group minerals. *Geol. Assoc. Can. – Mineral. Assoc. Can., Program Abstr.* **10**, A17.

_____, _____ & _____ (1993): Cesstibtantite – a geologic introduction to the inverse pyrochlores. *Mineral. Petrol.* **48**, 235-255.

_____, _____ & SIIVOLA, J. (1987): The composition of stannomicrolite. *Neues Jahrb. Mineral., Monatsh.*, 249-252.

_____, HAWTHORNE, F.C. & ČERNÝ, P. (1994): The structural chemistry of kalipyrochlore, a "hydropyrochlore". *Can. Mineral.* **32**, 415-420.

FOURQUET, J.L., JACOBINI, C. & DE PAPE, R. (1973): Les pyrochlores A'B₂O₆: mise en evidence de l'occupation par le cation A' de nouvelles positions cristallographiques dans le groupe d'espace Fd3m. *Mat. Res. Bull.* **8**, 393-404.

GOROGOTSKAYA, L.I., LITVIN, A.L., OSTAPENKO, S.S. & VOLOSHIN, A.L. (1996): Crystal structure of cesstibtantite. *Mineral. Zh.* **18**, 9-13 (in Russ.).

GROULT, D., PANNETIER, J. & RAVEAU, B. (1982): Neutron diffraction study of the defect pyrochlores $TaWO_{5.5}$, $HTaWO_3$, $H_2Ta_2O_6$, and $HTaW_6 \cdot H_2O$. *J. Solid State Chem.* **41**, 277-285.

HARRIS, P.M. (1965): Pandaite from the Mrima Hill niobium deposit (Kenya). *Mineral. Mag.* **35**, 277-290.

JÄGER, E., NIGGLI, E. & VAN DER VEEN, A.H. (1959): A hydrated barium–strontium pyrochlore in a biotite rock from Panda Hill, Tanganyika. *Mineral. Mag.* **32**, 10-25.

LANGHOF, J. & HOLTSTAM, D. (1994): Boron-bearing chiavennite and other late-stage minerals of the Proterozoic lithium-pegmatites of Utö, Stockholm, Sweden. *Abstr., 16th Gen. Meeting, Int. Mineral. Assoc.* (*Pisa*), 232.

LUMPKIN, G.R. (1989): *Alpha-Decay Damage, Geochemical Alteration, and Crystal Chemistry of Natural Pyrochlores.* Ph.D. thesis, Univ. New Mexico, Albuquerque, New Mexico.

_____, CHAKOUMAKOS, B.C. & EWING, R.C. (1986): Mineralogy and radiation effects of microlite from the Harding pegmatite, Taos County, New Mexico. *Am. Mineral.* **71**, 569-588.

_____ & EWING, R.C. (1992): Geochemical alteration of pyrochlore group minerals: microlite subgroup. *Am. Mineral.* **77**, 179-188.

_____ & _____ (1995): Geochemical alteration of pyrochlore group minerals: pyrochlore subgroup. *Am. Mineral.* **80**, 732-743.

NICKEL, E.H. & ROBINSON, B.W. (1985): Kimrobinsonite, a new tantalum mineral from western Australia, and its association with cesstibtantite. *Can. Mineral.* **23**, 573-576.

NOVÁK, M. & ŠREIN, V. (1998): Niobian cesstibtantite from the Dobrá Voda lepidolite pegmatite, western Moravia, Czech Republic. *Neues Jahrb. Mineral., Monatsh.*, 354-360.

OHNENSTETTER, D. & PIANTONE, P. (1992): Pyrochlore-group minerals in the Beauvoir peraluminous leucogranite, Massif Central. France. *Can. Mineral.* **30**, 771-784.

POUCHOU, J.L. & PICHOIR, F. (1985): "PAP"(phi-rho-z) procedure for improved quantitative microanalysis. *In* Microbeam Analysis (J.T. Armstrong, ed.). San Francisco Press, San Francisco, California (104-106).

SMEDS, S.-A. & ČERNÝ, P. (1989): Pollucite from the Proterozoic petalite-bearing pegmatites of Utö, Stockholm archipeiago, Sweden. *Geol. Fören. Stockholm Förh.* **111**, 361-372.

TEERTSTRA, D.K., ČERNÝ, P. & HAWTHORNE, F.C. (1998): Rubidium feldspars in granitic pegmatites. *Can. Mineral.* **36**, 483-496.

_____. _____, LANGHOF, J., SMEDS, S.A. & GRENSMAN, F. (1996): Pollucite in Sweden: occurrences, crystal chemistry, petrology and subsolidus history. *GFF* **118**, 361-372.

VOLOSHIN, A.V., MEN'SHIKOV, YU.P., PAKHOMOVSKII, YA.A. & POLEZHAEVA, L.I. (1981): Cesstibtantite, (Cs,Na)SbTa$_4$O$_{12}$ – a new mineral from granitic pegmatites. *Zap. Vses. Mineral. Obshchest.* **116**, 345-351 (in Russ.).

_____, PAKHOMOVSKII, YA.A., BULGAK, L.V. & PERLINA, G.A. (1985): Ungursaite – a new tantalate of calcium and sodium from granitic pegmatites. *Mineral. Zh.* **7**, 88-94 (in Russ.).

_____, _____ & TYUSHEVA, F.M. (1982): Calciotantite, CaTa$_4$O$_{11}$, a new mineral from granitic pegmatites of the Kola Peninsula. *Mineral. Zh.* **4**, 75-79 (in Russ.).

WISE, M.A. & ČERNÝ, P. (1990): Primary compositional range and alteration trends of microlite from the Yellowknife pegmatite field, Northwest Territories, Canada. *Mineral. Petrol.* **43**, 83-98.

YAMNOVA, N.A., PUSHCHAROVSKII, D.Y. & VOLOSHIN, A.V. (1988): Identity of ungursaite with calciotantite and synthetic CaTa$_4$O$_{11}$. *Sov. Phys. Crystallogr.* **33**, 498-499.